A locally smoothed terrain-following vertical coordinate to improve the simulation of fog and low stratus in numerical weather prediction models

Stephanie Westerhuis[1,2], **Oliver Fuhrer**[2,3]

[1]ETH Zürich

[2]MeteoSwiss

[3]Vulcan Inc.

Key Points:

- Terrain-following vertical coordinates feature sloping vertical coordinate surfaces in the atmospheric boundary layer.
- Spurious numerical diffusion associated with advection across sloping vertical coordinate surfaces promotes erroneous dissipation of fog and low stratus.
- Local smoothing of the vertical coordinate surfaces improves forecasts of fog and low stratus.

Corresponding author: Stephanie Westerhuis, `stephanie.westerhuis@usys.ethz.ch`

Abstract

The correct simulation of fog and low stratus (FLS) is a difficult task for numerical weather prediction (NWP) models. The Swiss Plateau experiences many days with FLS in winter. Most NWP models employ terrain-following vertical coordinates. As a consequence, the typically flat cloud top is intersected by sloping coordinate surfaces above hilly terrain such as the Swiss Plateau. Horizontal advection across the sloping coordinate surfaces leads to spurious numerical diffusion which promotes erroneous FLS dissipation. To address this problem, we propose a new vertical coordinate formulation which features a local smoothing of the model levels. We demonstrate the positive impact of the new vertical coordinate formulation on a case study in detail and for a full month using the COSMO model. The improved vertical coordinate formulation is not yet sufficient to obtain perfect FLS forecasts, it is however a crucial aspect to consider on the way thereto.

Plain Language Summary

In Switzerland, the Swiss Plateau is prone to occurrence of fog and low stratus clouds (FLS) in winter. High-resolution weather prediction models are an important tool to predict FLS. However, they often struggle to provide accurate FLS forecasts. Among other model aspects which need to be improved, one issue is the determination of the computational mesh: Most weather models employ a mesh which follows the terrain at the Earth's surface, leading to grid cells that are tilted with respect to the horizontal at altitudes where FLS occur. The structure as well as the top of a FLS layer typically is horizontal. Thus, the cells of the computational mesh are at an angle with respect to the dominant physical processes that the model has to represent. We show that a sloping mesh is detrimental for the forecasting of FLS since it promotes premature dissipation of the clouds. For a widely used weather model, we propose a new way to determine the computational mesh leading to a smoother and flatter computational mesh over the Swiss Plateau. The model is still not able to yield perfect FLS forecasts, but in some cases the use of the new mesh leads to considerable forecast improvements.

1 Introduction

Despite many advancements in recent years, numerical weather prediction (NWP) models have low skill in forecasting fog and low stratus (FLS) (e.g., Tudor, 2010; Steeneveld & de Bode, 2018; Román-Cascón et al., 2019). Previous studies have addressed various model components, such as the microphysics parameterisation (Müller et al., 2010; Szintai et al., 2014), the turbulence parameterisation (Wilson & Fovell, 2018; Chachere & Pu, 2019; Pithani et al., 2019), the vertical grid spacing (Tardif, 2007; Philip et al., 2016) and the horizontal resolution (Boutle et al., 2016).

To our knowledge, no study on FLS modeling has yet addressed the choice of the vertical coordinate transformation. Most operational NWP models employ a terrain-following vertical coordinate system. One of the first was developed by Phillips (1957); he introduced the σ-coordinate with $\sigma = p/p_s$, p being the pressure and p_s the surface pressure. Similarly, Gal-Chen and Somerville (1975) proposed a terrain-following coordinate based on height. Terrain-following coordinate systems have the advantages that the wind component perpendicular to the model level vanishes at the bottom of the atmosphere and that the coupling to column-based physical parameterisations is straightforward.

So-called hybrid coordinate systems change from one coordinate transformation to another to retain advantages of both. Bleck (1978) was the first to use a hybrid coordinate, combining a terrain-following σ-coordinate in the boundary layer with an isentropic coordinate aloft. A challenging aspect of hybrid coordinate systems is to perform the coordinate transition as smoothly as possible (Simmons & Burridge, 1981).

A good vertical coordinate transformation is able to transition rapidly to smooth model levels away from the Earth's surface. This constraint has to be balanced with other constraints such as the smoothness of horizontal and vertical metric terms and limits on how thin model levels should become. Smooth model levels are desirable to alleviate various problems related to sloping coordinate surfaces: Inaccurate calculation of the horizontal pressure gradient (Mahrer, 1984; Mesinger & Janjić, 1985; Zängl, 2012), inconsistent treatment of the metric terms (Klemp, 2011), and unphysical impacts of explicit horizontal diffusion (Zängl, 2002). In previous studies on FLS modeling, we have shown that horizontal advection schemes exhibit erroneous implicit numerical diffuson in a coordinate system with sloping vertical coordinate surfaces.

This diffusive behaviour results in excessive vertical mixing across the cloud top, promoting premature FLS dissipation (Westerhuis, Fuhrer, Bhattacharya, et al., 2020; Westerhuis, Fuhrer, Cermak, & Eugster, 2020).

To attain a fast decay of the orographic signal with height, Schär et al. (2002) have introduced the Smooth LEvel VErtical coordinate (SLEVE, generalised by Leuenberger et al., 2010). SLEVE allows for smooth coordinate surfaces at mid- and upper-levels by splitting the orography into a large- and a small-scale part with two different decay constants. Idealised tests simulating horizontal advection of moist bubbles several kilometers above the ground show that numerical errors are largely reduced when using a vertical coordinate formulation which exhibits less sloping vertical coordinates (Schär et al., 2002; Zängl, 2003). Klemp (2011) has proposed a different approach than SLEVE: Direct smoothing of the vertical coordinate surfaces by applying a smoothing operator. The strength of the filter, specifically the smoothing coefficient, progressively increases with altitude.

However, both SLEVE and Klemp's vertical coordinate formulation focus on attaining smooth levels at elevations much higher than where FLS typically occur. In both approaches, the model levels are smoothed equally irrespective of the amplitude of the underlying orography. Taking the example of Switzerland (Figure 1), FLS occur mostly on the Swiss Plateau, a region where the orography consists of gentle hills. But the adjacent Alps comprising high peaks and deep valleys determine the maximum amount of smoothing of the model levels aloft. Taking advantage of the fact that the vertical coordinate surfaces in certain regions can be smoothed much more aggressively, we propose a LOcally Smoothed VErtical Coordinate (LOSVEC), and show its impact on FLS forecasts.

We give details about the model and LOSVEC in Section 2. We present a detailed analysis of a single case study and verification scores for a one-month period in Section 3. The discussion of these results and suggestions for improvements of the vertical coordinate follow in Section 4. We summarise our findings in Section 5.

2 Model description

The simulations presented in this work are conducted with the COSMO model (version 5.0), which is developed by the COnsortium for Small-scale MOdelling. Our

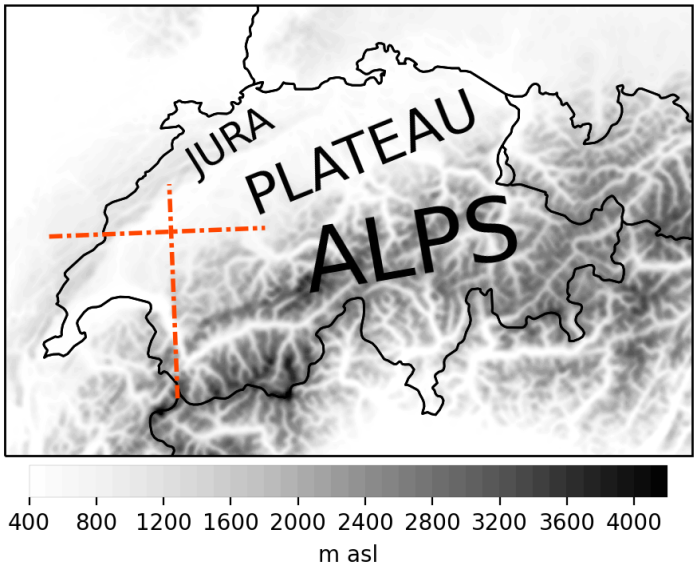

Figure 1. COSMO-1 model orography of Switzerland and surroundings. The Swiss Plateau is confined by the Jura Mountains in the north and the Alps in the south. The dash-dotted lines indicate the cross-sections shown in Fig. 2, they intersect at Payerne.

configuration follows COSMO-1, the deterministic model version with 1.1 km horizontal grid spacing which is employed operationally at MeteoSwiss, the Federal Office of Meteorology and Climatology in Switzerland. COSMO-1 spans the full Alpine region. The boundaries are derived from the Integrated Forecasting System employed at the European Centre for Medium-Range Weather Forecasts. The simulations are started from analyses obtained from a continuous observation assimilation cycle; horizontal winds, surface pressure, temperature, and humidity measurements are assimilated employing a nudging algorithm (Schraff & Hess, 2012).

The COSMO model solves the nonhydrostatic, fully compressible, hydro-thermodynamical equations of motion with finite-difference methods on an Arakawa C-grid (Arakawa & Lamb, 1977; Steppeler et al., 2003; Förstner & Doms, 2004). In the horizontal, the governing equations are discretised on a rotated latitude-longitude grid. In the vertical, a hybrid-version of the SLEVE coordinate (Schär et al., 2002; Leuenberger et al., 2010; Doms & Baldauf, 2013) is employed consisting of 80 model levels; the decay constants for large- and small-scale orographic features are set at $s1$ =10,000 m and $s2$=3,300 m, respectively. The elevation above which the orographic signal has de-

cayed completely is set at 11,357 m above sea level (asl). The lowest model half-level is located approximately 10 m above the ground, the model top is at 22,000 m asl.

A third-order Runge-Kutta discretisation with time-splitting for slow and fast processes integrates the prognostic variables forward in time (Klemp & Wilhelmson, 1978; Wicker & Skamarock, 2002). Horizontal advection of wind velocity, temperature and pressure is calculated with a fifth-order advection scheme. In the vertical, a second-order implicit Crank-Nicholson scheme is employed (Baldauf et al., 2011). Moist quantities (water vapour, cloud water, cloud ice, rain, snow, and graupel) are advected with a second-order positive-definite advection scheme with directional splitting (Bott, 1989; Schneider & Bott, 2014).

Turbulent fluxes are estimated via K-theory, the turbulent diffusion coefficients are calculated with a prognostic TKE-based 1.5-order scheme (Raschendorfer, 2001) with a 2.5 closure following Mellor and Yamada (1974, 1982).

A single-moment bulk microphysics scheme describes conversions between the six moist quantities (Reinhardt & Seifert, 2006). Subgrid-scale cloudiness is diagnosed by a statistical method based on the saturation deficit (Sommeria & Deardorff, 1977). Radiative processes interacting with grid- and subgrid-scale clouds are described with a delta-two-stream approach (Ritter & Geleyn, 1992).

2.1 Formulation for locally smoothed vertical coordinate surfaces

As outlined above, LOSVEC attains a regionally varying vertical decay of the orographic signal. The main motivation for this approach is that for regions without extremely complex orography, a strong smoothing of the coordinate surfaces can be applied. Similarly to other options available for the COSMO model – height-based hybrid coordinates based on the Gal-Chen or the SLEVE coordinate – LOSVEC is formulated as a hybrid coordinate.

LOSVEC is constructed from the surface upwards. In the following, z refers to the elevation of a model surface and Δz to the height difference between two model surfaces. Each level undergoes two steps: First, to attain a hybrid coordinate formulation, an initial z is chosen such that the levels become flat at a specific elevation (11,357 m asl in COSMO-1, see Appendix for details). In a second step, a two-dimensional diffusion

operator is applied, similar as in Klemp (2011). At a grid point with the indices i, j the following calculation is conducted (the level index k is omitted for easier readability):

$$\begin{aligned}\hat{z}_{i,j} = z_{i,j} - c_{i,j}\Big[&\frac{3}{4}z_{i,j} \\ &+ \frac{1}{16}\big(z_{i-1,j-1} + z_{i-1,j+1} + z_{i+1,j-1} + z_{i+1,j+1}\big) \\ &+ \frac{1}{8}\big(z_{i-1,j} + z_{i+1,j} + z_{i,j-1} + z_{i,j+1}\big)\Big]\end{aligned} \tag{1}$$

The smoothing coefficient is small ($c_{i,j} = 0.01$), but the filter is applied multiple times ($N_{ITER} = 100$, unless denoted otherwise). To attain a local smoothing, a set of constraints switches the filter off, i.e. overriding $c_{i,j} = 0$, at grid points where $\Delta\hat{z}$ would become too small or too large, at each filter iteration.

Various combinations of filter constraints have to be tested to find a good compromise between ensuring smooth coordinate surfaces in the horizontal while maintaining smooth Δz distributions in the vertical. For the simulations presented in this study, two constraints are applied to ensure a minimal level thickness of $\Delta z_{MIN} = 15\,\mathrm{m}$ and to prevent an exaggerated increase in level thickness, $c_{INF} = 1.8$:

1. $\Delta\hat{z} > \Delta z_{MIN}$
2. $\Delta\hat{z} < c_{INF}\Delta z$

Figure 2 displays cross-sections through Payerne (location is indicated in Figure 1) in both directions for the 24 lowest model levels. LOSVEC (Panels b and c) exhibits much smoother coordinate surfaces than SLEVE (Panels a and d). As a consequence of the diffusion filter, the levels above depressions such as the Rhône Valley are significantly thicker in LOSVEC compared to SLEVE, while those above the Alpine peaks are thinner. On the Swiss Plateau, the small-scale structures from the hilly orography decay quickly in LOSVEC.

Power spectral densities (PSDs) describe a decomposition of a field into a range of spatial frequencies (Jacobs et al., 2017). Analysis of the PSDs of coordinate surfaces of SLEVE and LOSVEC allows for a quantitative comparison between the two vertical coordinate formulations. Figure 3 shows the PSDs calculated in the zonal direction of the raw 1-km-grid orography, the filtered orography as it is used in the COSMO model, and the 20th coordinate surface of both, SLEVE and LOSVEC. The PSDs in the meridional direction look alike, but are not shown here.

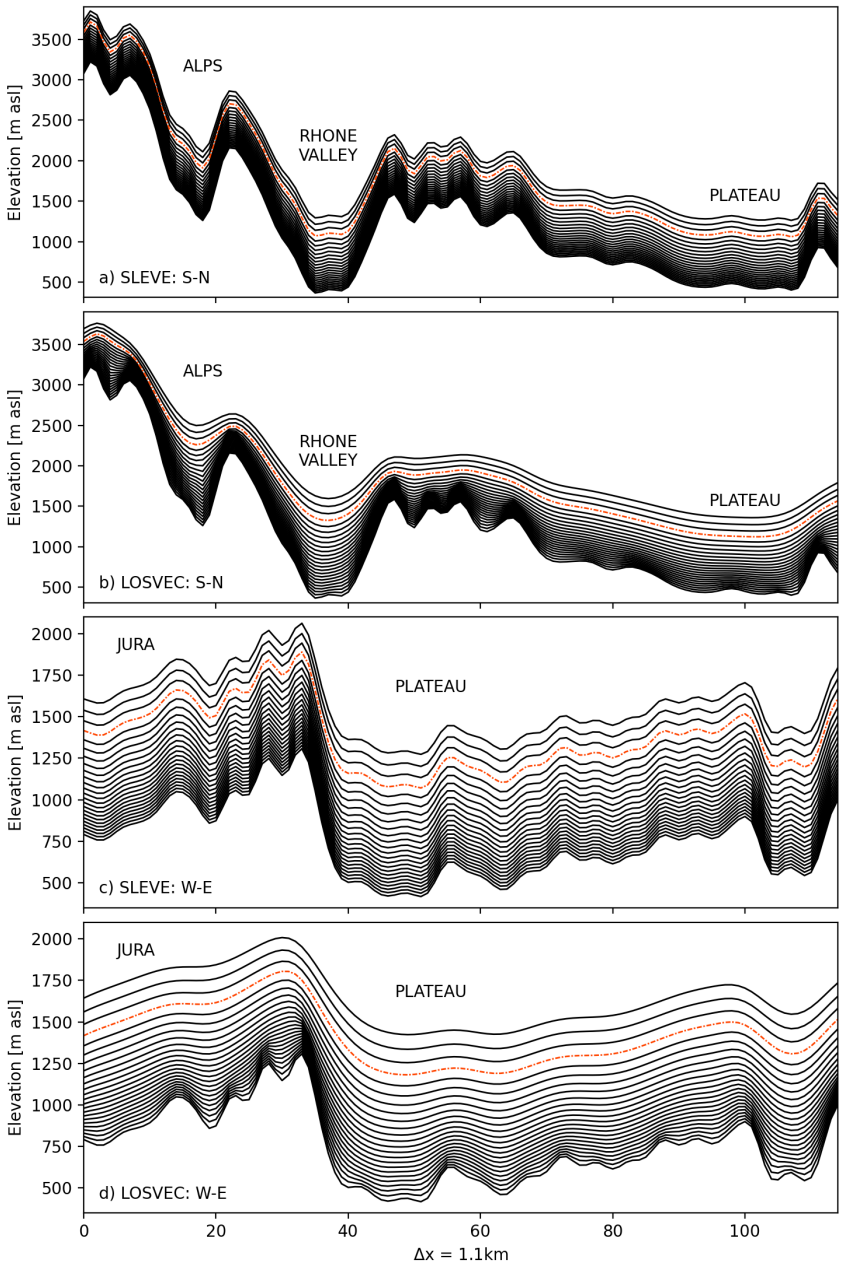

Figure 2. Cross-sections of the lowest 24 model levels for SLEVE (a and c) and LOSVEC (b and d) in S-N and W-E direction. The locations of the cross-sections are indicated in Fig. 1. The power spectral densities of the 20th level, drawn as a dash-dotted line, are shown in Fig. 3.

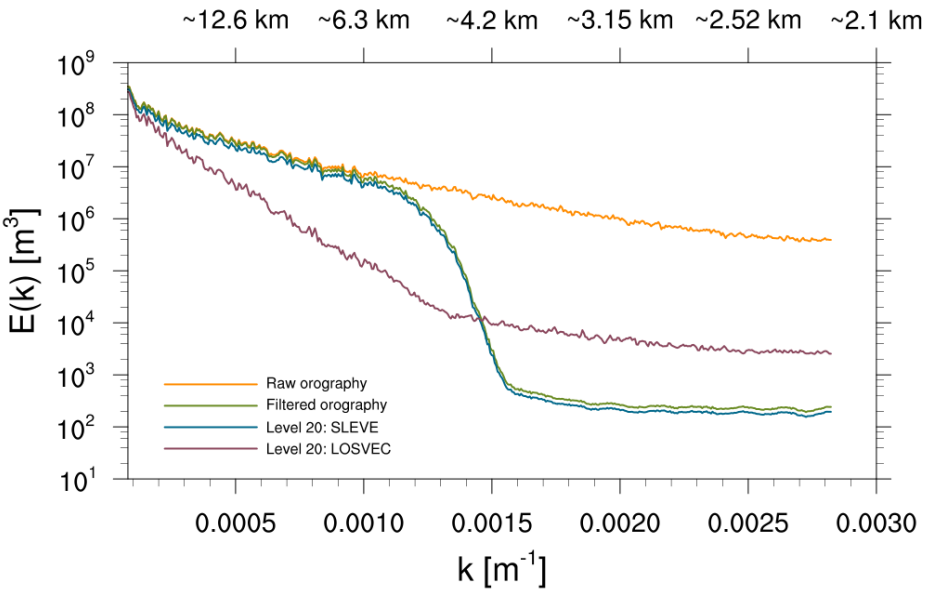

Figure 3. Power spectral density computed for the raw orography (orange), filtered orography (green), level 20 of SLEVE (blue), level 20 of LOSVEC (purple) in the zonal direction.

The raw orography (orange line) is based on the digital elevation map provided by the Advanced Spaceborne Thermal Emission and Reflection Radiometer (ASTER). Before being used by the NWP model, the topography is smoothed using a low-pass filter (Raymond, 1988) with a cut-off of about 4-5 Δx (green line). In a terrain-following vertical coordinate, the orographic signal decays with height. However, the PSD of the 20th coordinate surface using the SLEVE vertical coordiante indicates that only very little smoothing has occurred (as compard to the orography). This is a consequence of the formulation of this vertical coordinate which focuses on obtaining smooth levels at mid-levels and aloft. In Westerhuis, Fuhrer, Bhattacharya, et al. (2020) we have shown that sloping vertical coordinates at scales $> 5\Delta$x promote spurious numerical diffusion at the cloud top of an idealised stratus cloud. Unlike SLEVE, LOSVEC is able to considerably remove power at these scales at levels close to the surface (purple line). The increase in power at small scales is likely a consequence of the filter constraints being active over very steep topography.

3 Results: FLS simulations

3.1 Case study: December 29, 2016

On the days around December 29, 2016, a high pressure system north of Switzerland led to northeasterly winds on the Swiss Plateau, so-called Bise (Wanner & Furger, 1990). Typically, Bise is related to cold-air advection which favors continuous cold air pooling on the Swiss Plateau. On December 28, the first few small FLS patches developed. During the night of December 28–29, a large part of the air mass on the Swiss Plateau reached its dewpoint temperature and wide-spread FLS formed. The cloud dissipated again in the afternoon of December 29.

Figure 4 compares satellite observations with the liquid water path forecasted by two COSMO-1 simulations initialised on December 28, 12 UTC, employing SLEVE and LOSVEC, respectively. Both configurations generally underpredict FLS on the Swiss Plateau (not in the region of the Rhine valley in Germany though). However, with LOSVEC, the model simulates more extensive FLS than with SLEVE. Especially at 09 UTC, the forecasted FLS extent is considerably more accurate with LOSVEC: The SLEVE simulation has has largely dissipated the FLS on the Swiss Plateau while the LOSVEC simulation still features extensive FLS.

Interestingly, the localisation of the FLS is relatively accurate for both configurations, the fine-scale FLS structure such as the extension into the small valleys extending southwards is surprisingly well represented as well as the delimitation at the eastern and western edge. The underestimation and too early dissipation of the FLS on the Swiss Plateau clearly are the main issues here. The extent of the FLS occurring further north in the Rhine valley is simulated similarly in both configurations. This region is dominated by less distinct topography than the Swiss Plateau, hence sloping vertical coordinate surfaces are less critical.

Figure 5 shows the vertical profiles above Payerne (location indicated in Figure 1) of temperature, wind speed, specific humidity and the liquid water content (LWC) simulated by COSMO-1 with either SLEVE (solid line), or LOSVEC (dashed line). We display the profiles on December 29 at 00 UTC, 06 UTC and 12 UTC. Except for the LWC, where the profiles at midnight and noon do not exhibit any LWC and are therefore replaced by the profiles of 03 UTC and 09 UTC, respectively. Twice a day,

balloon radiosoundings are launched at Payerne; the measured values are shown as dotted lines.

At midnight (12 hours into the model simulations), a cool and moist air mass lies on the Swiss Plateau and is capped by a temperature inversion at around 900 m asl (a). The air is mostly well-mixed except for a shallow surface inversion. Both model configurations underestimate the vertical extent of the cool air mass and fail to reproduce the shallow temperature inversion close to the surface but exhibit constantly increasing temperature from the ground upwards instead.

A low-level jet reaches maximum wind speeds of about 7 m/s at 50 m above the ground (d). At the height of the temperature inversion, the Bise attains 8 m/s. Neither of the model simulations features this low-level jet but both exhibit considerable wind at around 900 m asl. The lower atmosphere in the model is clearly affected by the Bise and hence subject to horizontal advection.

Horizontal advection of humidity tracers in a vertical coordinate system exhibiting sloping coordinate surfaces leads to spurious numerical diffusion resulting in excessive vertical mixing (Westerhuis, Fuhrer, Bhattacharya, et al., 2020). The specific humidity profiles illustrate this point: In reality, the lower atmosphere consists of a moist air mass with a specific humidity of about 3 g/kg (g and i). In the model analyses of December 28, 12 UTC, this moist layer is well represented (not shown), but with increasing model leadtime the humidity gets progressively mixed with dryer air from aloft. This process is however reduced with LOSVEC compared to SLEVE.

The LOSVEC configuration is able to form a cloud extending up to 750 m asl while the cloud simulated with the SLEVE configuration remains very shallow (j,k,l). As a consequence of the more extensive cloud, the LOSVEC simulation experiences stronger radiative cloud top cooling which in turn leads to a more prominent temperature inversion at 06 UTC and 12 UTC (b and c).

The impact of the smoothing of the coordinate surfaces is further illustrated in Figure 6. It displays vertical profiles of the LWC and the total humidity (sum of LWC and specific humidity) above Payerne at 03 UTC, i.e. 15 hours into the simulation, for five different model configurations: SLEVE and LOSVEC constructed with 0, 10, 50, and 100 filter iterations. More filter iterations, i.e. smoother vertical coordinate

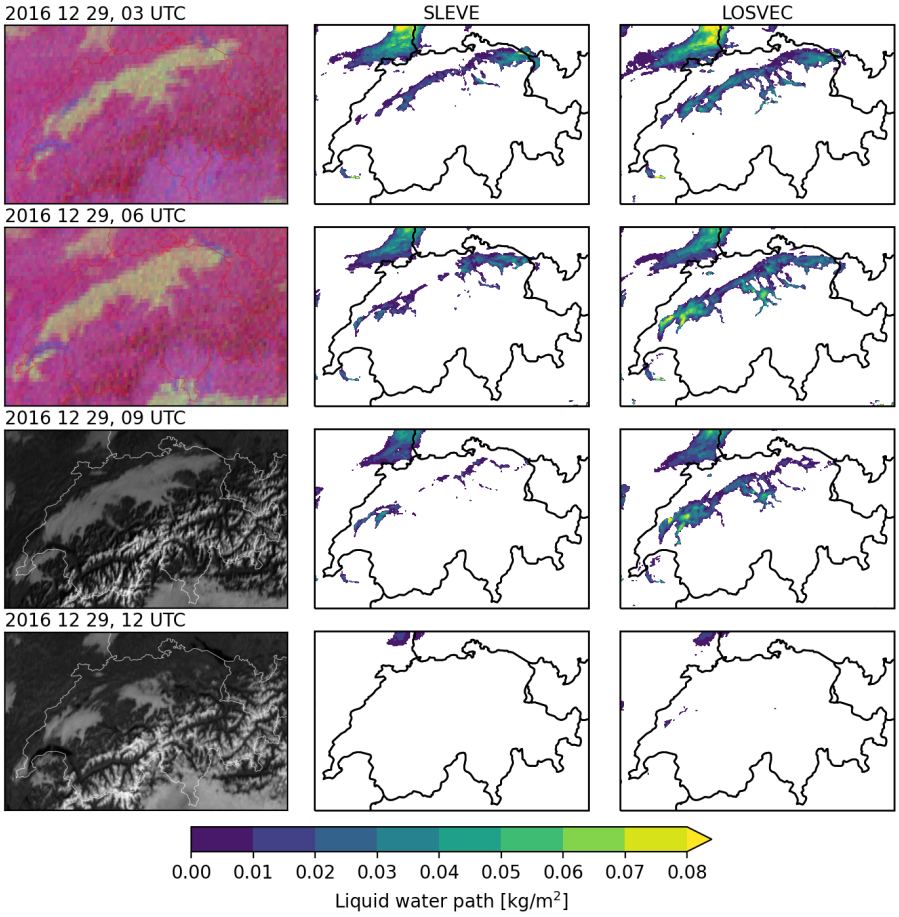

Figure 4. FLS on December 29, 2016. Satellite observations (yellow and grey areas in the left panel), COSMO-1 forecasts with SLEVE (middle panel) and LOSVEC (right panel). With LOSVEC, the forecasted FLS extent is larger and hence more accurate, however, both model configurations dissipate the clouds too early.

surfaces, are associated with higher total humidity in the lowest atmospheric layers and a more extensive cloud.

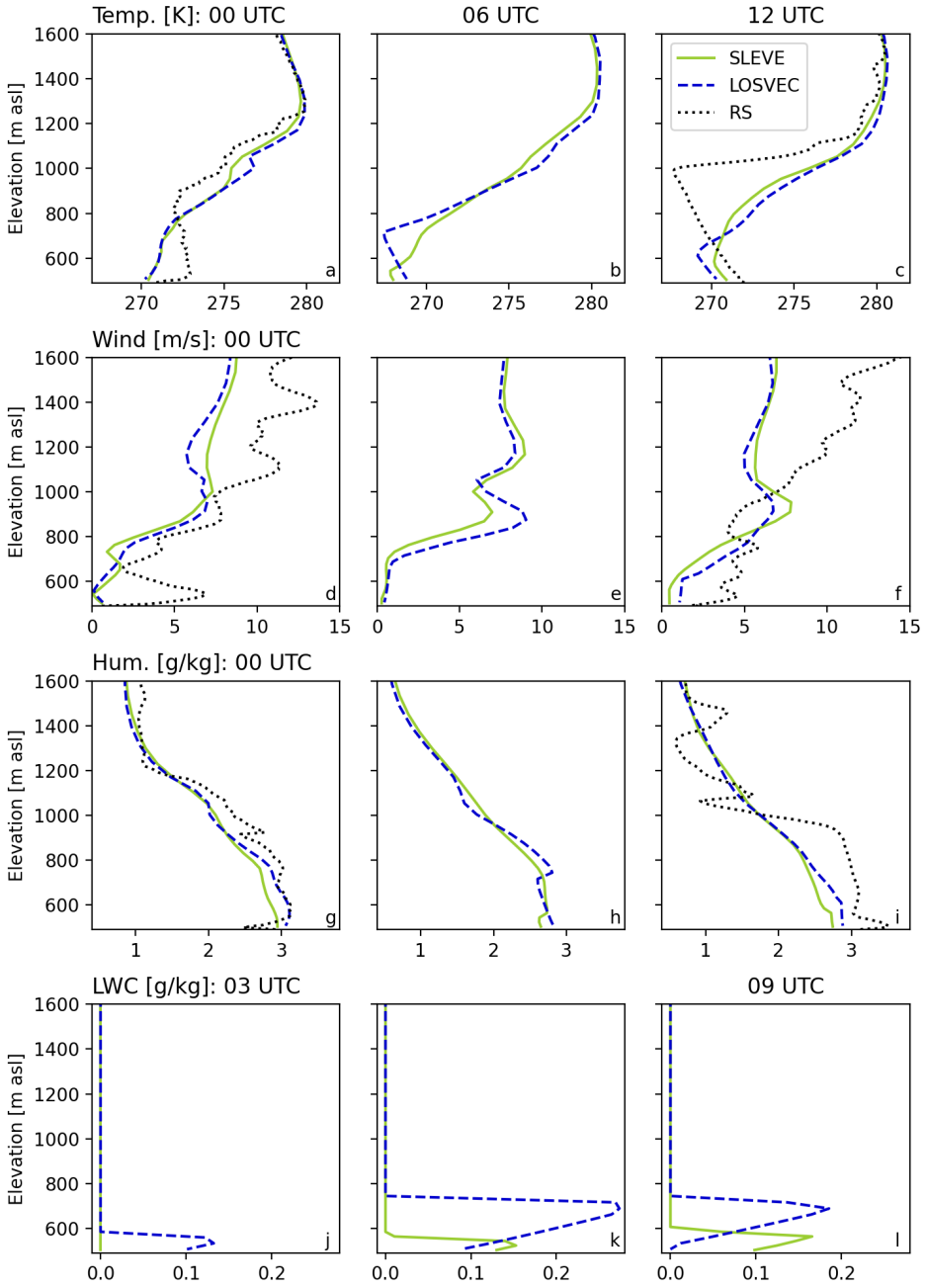

Figure 5. Vertical profiles of temparature, wind speed, specific humidity and LWC above Payerne on December 29, 2016: Balloon radiosounding measurements (dotted lines), COSMO-1 simulations initialised on December 28, 12 UTC, with SLEVE (solid line), or LOSVEC (dashed lines).

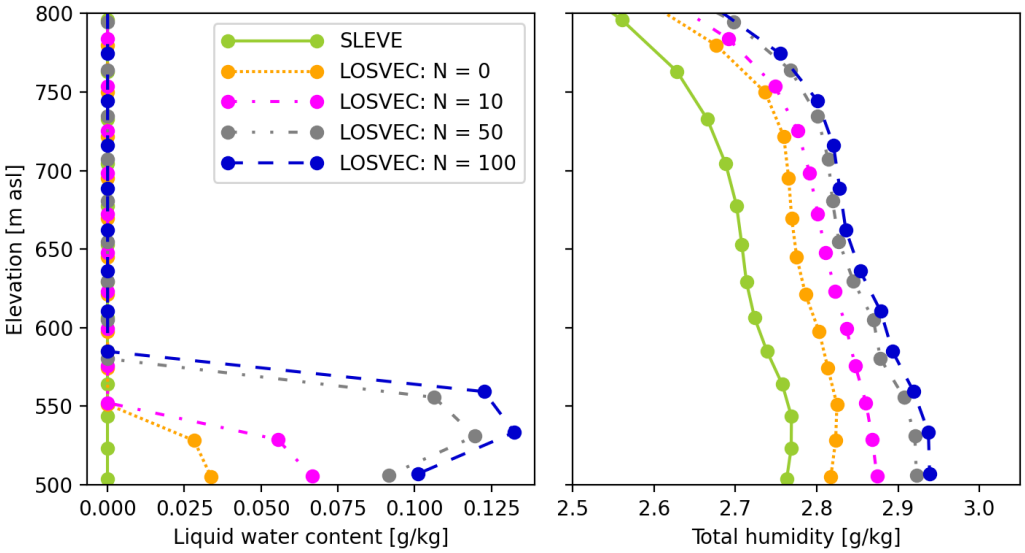

Figure 6. Vertical profiles of LWC and total humidity (sum of LWC and specific humidity) above Payerne on December 29, 2016, 03 UTC, simulated with COSMO-1. The simulations are initialised on December 28, 2016, 12 UTC and only differ by the vertical coordinate systems employed: SLEVE, or LOSVEC constructed with 0, 10, 50, 100 iterations of the diffusion filter applied to the coordinate surfaces.

3.2 Satellite-based verification of a full month

In December 2016, many periods with persistent FLS occurred on the Swiss Plateau. Hence, this month constitutes an ideal period to evaluate FLS forecasts on a longer timescale. Twice a day, at 00 UTC and 12 UTC, we start 24-hour forecasts from an analysis retrieved from a continuous data assimilation cycle. (The data assimilation ensures that model errors do not affect subsequent simulations.) We evaluate forecasts of COSMO-1 using either SLEVE or LOSVEC for the full month with a satellite-based verification algorithm. The details for the algorithm are described in Westerhuis, Fuhrer, Cermak, and Eugster (2020), we briefly outline the procedure in the following.

The basic idea is to compare the extent of the area covered by FLS. The location of the FLS is neglected – it is of secondary importance as the structure of FLS is often predetermined by the orography of the Swiss Plateau. For both, the satellite observations and the model forecasts, each grid point in a predefined area comprising the Swiss Plateau is classified as either being covered by FLS or not covered by FLS.

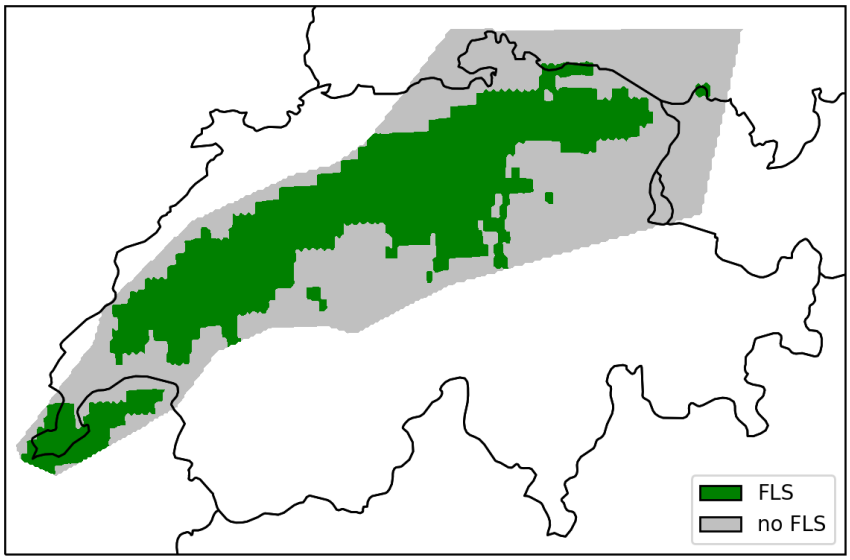

Figure 7. Satellite observations classifying whether a grid point in an area comprising the Swiss Plateau is covered by FLS or not on December 29, 2016, 09 UTC. In total, 42 % of the contemplable grid points are covered by FLS.

Finally, the fraction of grid points covered by FLS is compared. The choice of area of interest directly affects this fraction, it is only useful when set into contrast with FLS grid point fractions derived for the same area.

For the presented case study, on December 29, 2016, 09 UTC, the satellite observations indicate a FLS grid point fraction of 0.42, illustrated in Figure 7. The forecasts issued 21 hours earlier exhibit FLS fractions of 0.06 (SLEVE) and 0.2 (LOSVEC), respectively. Even though COSMO-1 with LOSVEC misses about half of the FLS covered grid points, the simple spatial verification algorithm points out that this configuration performs clearly better than COSMO-1 with SLEVE.

Considering satellite observations every 3 hours during December 2016, excluding days with high clouds (more than 10% of grid points) or negligible FLS occurrence (less than 20% of grid points), results in a dataset comprising 117 observations. (The results are not very sensitive to the selection of these thresholds.)

For the selected observations, the median FLS fraction is 0.53, ranging from 0.46 (at 18 UTC) to 0.59 (at 06 UTC). Figure 8 shows the median FLS fractions forecasted by COSMO employing SLEVE (light bars) and LOSVEC (dark bars), respectively,

for increasing leadtime. The whiskers represent the interquartile range. The median observed FLS fraction is indicated with the horizontal line at the top.

Regardless of the vertical coordinate formulation employed, both COSMO simulations heavily underestimate the FLS. The underestimation gets worse with increasing leadtime. However, at all leadtimes after the analysis, the configuration with LOSVEC consistently exhibits more FLS. Although the differences are small they appear statistically significant in a paired t-test.

A closer investigation of the forecasts shows that there are many cases where the configurations are similar and several where LOSVEC is clearly better, such as the presented case study. Among all forecasts which underestimate FLS on the Swiss Plateau (FLS fraction bias $<$ -0.05), 33 lead time instances from 18 different forecasts stand out for which the simulation employing LOSVEC instead of SLEVE is discernibly better (difference in FLS fraction $>$ 0.05). Only 3 leadtime instances from 2 different forecasts using SLEVE are perceivably better. The subjectively selected threshold of 0.05 relates to differences in area covered by FLS distinguishable by eye, e.g. by a forecaster.

To summarise, LOSVEC is not able to completely resolve the notorious underestimation of FLS on the Swiss Plateau with the COSMO model. However, employing LOSVEC instead of SLEVE clearly improves a fair number of forecasts.

4 Discussion

Our results imply that a careful re-formulation of the vertical coordinate is able to improve FLS forecasts issued by a high-resolution numerical weather prediction model. Previous studies have demonstrated increased accuracy for model configurations employing smoothed coordinate surfaces focusing on the middle troposphere (Schär et al., 2002; Zängl, 2003; Klemp, 2011). For idealised simulations of a stratus cloud close to the surface, we have already shown in Westerhuis, Fuhrer, Bhattacharya, et al. (2020) that sloping vertical coordinate surfaces cause spurious numerical diffusion in cases where horizontal advection occurs. With LOSVEC we are able to alleviate these issues. A noteworthy aspect hereby is that introducing a new vertical coordinate formulation is not associated with an increase in computational costs. Furthermore,

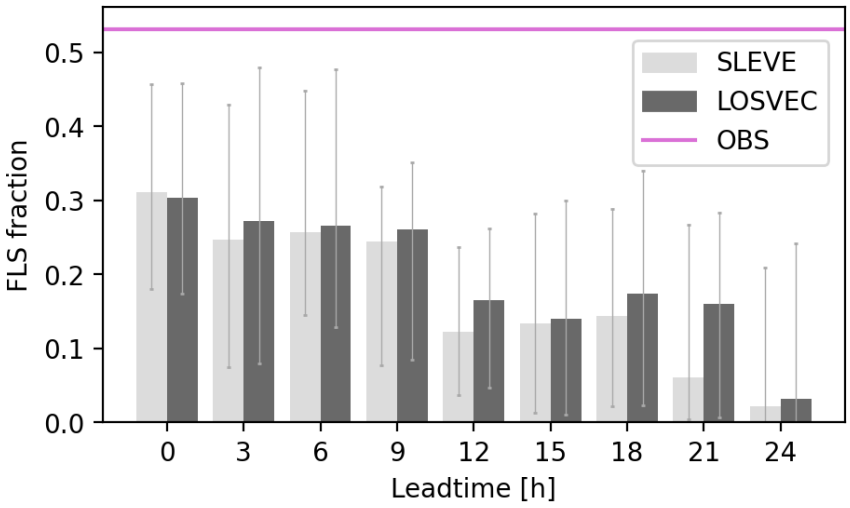

Figure 8. Median fraction of grid points comprising the Swiss Plateau which is covered by FLS during December 2016: Observed (horizontal line), forecasted by COSMO employing SLEVE (light coloured bars) or LOSVEC (dark coloured bars). The whiskers denote the interquartile range.

also other known issues, such as the calculation of the horizontal pressure gradient, may profit from less sloping vertical coordinate surfaces.

Tardif (2007) and Philip et al. (2016) have shown that increasing the vertical resolution improves FLS simulations. However, in our experiments, LOSVEC exhibits even slightly thicker model levels than SLEVE at low altitudes at most grid points. The positive impact of LOSVEC is hence not a consequence of reduced vertical grid spacing.

LOSVEC is easily transferable to any NWP model which employs a terrain-following vertical coordinate formulation. To ensure that LOSVEC is suitable for an operational NWP model, further tests should be conducted focusing on other atmospheric phenomena such as thunderstorms, valley winds, and frontal systems. Moreover, we are confident that additional testing addressing the initial z distribution (based on the reference level distribution, z_{REF}, see Appendix), as well as Δz_{MIN} and c_{INF} could provide an optimised version of LOSVEC. From a numerical viewpoint, smooth transitions of Δz with height are crucial for accurate calculations of the metric terms. Progressively adapting Δz_{MIN} and c_{INF} with altitude might allow for

a better compromise between smooth levels in the horizontal and smooth Δz in the vertical.

Clearly, smoothing the vertical coordinate surfaces is not a sufficient measure to attain perfect FLS forecasts. The FLS life cycle is governed by a delicate balance of many different processes subject to non-linear interactions. Perfect initial conditions, accurate physical parameterisations and a correct representation of the underlying soil are also crucial for successful representation of FLS in NWP models (e.g., Steeneveld & de Bode, 2018). Our results however strongly indicate that a better choice of vertical coordinate transformation ensuring a fast decay of the orographic signal with altitude is one important element to consider in cases where horizontal advection cannot be neglected.

5 Summary

Forecasting fog and low stratus (FLS) poses a major challenge for state-of-the-art numerical weather prediction (NWP) models. We have developed a new vertical coordinate transformation for the COSMO model to reduce spurious numerical diffusion associated with sloping coordinate surfaces. We make use of the fact that within a model domain comprising variable topographic sub-regions, the vertical coordinate surfaces above flat and moderately hilly regions can be smoothed much more aggressively than in other regions comprising high mountains. The LOcally Smoothed VErtical Coordinate, LOSVEC, attains a fast decay of the orographic signal with altitude by applying a two-dimensional diffusion filter directly to the coordinate surfaces with a locally varying strength.

The new vertical coordinate is compared to the standard Smooth LEvel VErtical coordinate, SLEVE, for a case of wide-spread FLS on the Swiss Plateau. With LOSVEC, the model still underpredicts FLS on the Swiss Plateau, but it develops generally more extensive FLS and, as a consequence, generates the better forecast.

Evaluating the performances of both model configurations for a full month with many FLS days with a satellite-based verification algorithm confirms the findings from the case study: The COSMO model generally underpredicts FLS on the Swiss Plateau, however, with LOSVEC it is able to simulate more FLS than with SLEVE.

Before LOSVEC can be employed in an operational NWP model, it has to be refined and tested for other atmospheric phenomena. Our results nevertheless underline the importance of conducting research on vertical coordinates in the future.

Appendix A Calculation of z

The Gal-Chen and SLEVE hybrid coordinate formulations in the COSMO model feature a reference level distribution, z_{REF}, from 0 m asl to 22,000 m asl, for which Δz progressively increases. To attain a hybrid coordinate formulation, Δz of the model levels is compressed linearly between the surface, z_{SURF}, and a predefined elevation $z_{FLAT} = 11{,}357$ m asl. The thinnest level is thus located at the grid point with highest elevation.

To have a better control over the minimal Δz when smoothing the coordinate surfaces, we have reversed the calculation of z_{REF}: Instead of linearly compressing Δz below z_{FLAT} at all grid points with $z_{SURF} > 0$, the levels at all grid points below the highest grid point are inflated. In recursive form, the elevation of level k, z_k, is calculated like this:

$$z_k = z_{REF,k} - \frac{a_k}{a_{k-1}}(z_{REF,k-1} - z_{k-1}), \text{with} \tag{A1}$$

$$a_k = \frac{z_{FLAT} - z_{REF,k}}{z_{FLAT} - \max(z_{SURF})} \tag{A2}$$

The Δz distribution of the SLEVE levels around z_{FLAT} features a jump, as can be seen in Figure A1 which shows the Δz distribution at the highest and lowest point in the model domain (compare solid with dotted line). To avoid such features, which may be enhanced when applying the diffusion filter, we have adapted the basic Δz_{REF} distribution for LOSVEC, illustrated with the dashed and dash-dotted lines in Figure A1.

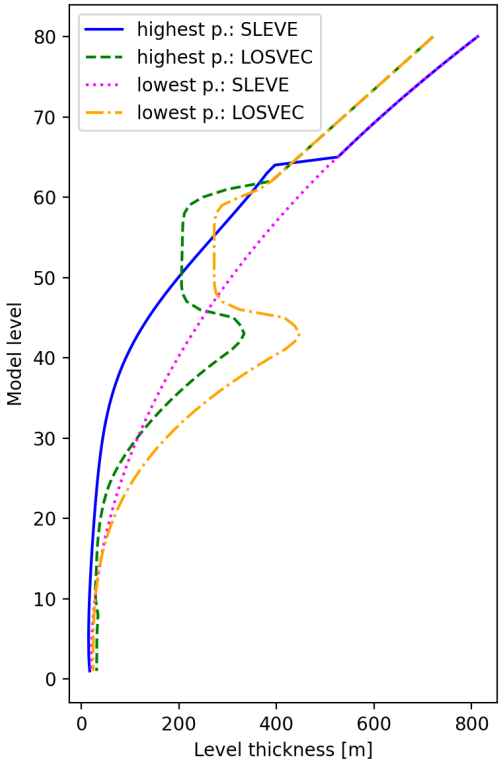

Figure A1. Δz of the SLEVE and LOSVEC model levels above the grid points with highest and lowest elevation, respectively. With SLEVE, the lowest 64 levels are compressed (solid line) compared to the level distribution starting at sea level (dotted line). With LOSVEC, the basic level distribution is defined at the highest grid point (dashed line) and at all other grid points the lowest 61 levels are stretched (dash-dotted line).

Acknowledgments

We thank Werner Eugster and Mathias Rotach for their feedback on an early version of the manuscript. We thank the Swiss National Supercomputing Centre (CSCS) for providing the computational resources. Stephanie Westerhuis is supported by ETH research grant ETH-17 16-2. The data used in this study are available at https://doi.org/10.5281/zenodo.4419639.

References

Arakawa, A., & Lamb, V. R. (1977). Computational design of the basic dynamical processes of the UCLA general circulation model. *General Circulation Models of the Atmosphere*, *17*(Supplement C), 173–265.

Baldauf, M., Seifert, A., Förstner, J., Majewski, D., Raschendorfer, M., & Reinhardt, T. (2011). Operational convective-scale numerical weather prediction with the COSMO model: Description and sensitivities. *Monthly Weather Review*, *139*(12), 3887–3905. doi: https://doi.org/10.1175/MWR-D-10-05013.1

Bleck, R. (1978). On the use of hybrid vertical coordinates in numerical weather prediction models. *Monthly Weather Review*, *106*(9), 1233–1244. doi: https://doi.org/10.1175/1520-0493(1978)106%3C1233:OTUOHV%3E2.0.CO;2

Bott, A. (1989). A positive definite advection scheme obtained by nonlinear renormalization of the advective fluxes. *Monthly Weather Review*, *117*(5), 1006–1016. doi: https://doi.org/10.1175/1520-0493(1989)117%3C1006:APDASO%3E2.0.CO;2

Boutle, I., Finnenkoetter, A., Lock, A., & Wells, H. (2016). The London Model: Forecasting fog at 333 m resolution. *Quarterly Journal of the Royal Meteorological Society*, *142*(694), 360–371. doi: https://doi.org/10.1002/qj.2656

Chachere, C. N., & Pu, Z. (2019). Numerical simulations of an inversion fog event in the salt lake valley during the MATERHORN-fog field campaign. *Pure and Applied Geophysics*, *176*(5), 2139–2164. doi: https://doi.org/10.1007/s00024-018-1770-8

Doms, G., & Baldauf, M. (2013). A description of the nonhydrostatic regional COSMO-model: Part I: Dynamics and numerics. *COSMO Documentation*. doi: 10.5676/DWDpub/nwv/cosmo-doc5.00I

Förstner, J., & Doms, G. (2004). Runge-Kutta time integration and high-order

spatial discretization of advection-a new dynamical core for the LMK. *COSMO Newsletter*, *4*, 168–176.

Gal-Chen, T., & Somerville, R. C. (1975). On the use of a coordinate transformation for the solution of the navier-stokes equations. *Journal of Computational Physics*, *17*(2), 209–228. doi: https://doi.org/10.1016/0021-9991(75)90037-6

Jacobs, T. D., Junge, T., & Pastewka, L. (2017). Quantitative characterization of surface topography using spectral analysis. *Surface Topography: Metrology and Properties*, *5*(1), 013001. doi: 10.1088/2051-672x/aa51f8

Klemp, J. B. (2011). A terrain-following coordinate with smoothed coordinate surfaces. *Monthly Weather Review*, *139*(7), 2163–2169. doi: https://doi.org/10.1175/MWR-D-10-05046.1

Klemp, J. B., & Wilhelmson, R. B. (1978). The simulation of three-dimensional convective storm dynamics. *Journal of the Atmospheric Sciences*, *35*(6), 1070–1096.

Leuenberger, D., Koller, M., Fuhrer, O., & Schär, C. (2010). A generalization of the SLEVE vertical coordinate. *Monthly Weather Review*, *138*(9), 3683–3689. doi: https://doi.org/10.1175/2010MWR3307.1

Mahrer, Y. (1984). An improved numerical approximation of the horizontal gradients in a terrain-following coordinate system. *Monthly Weather Review*, *112*(5), 918–922. doi: https://doi.org/10.1175/1520-0493(1984)112%3C0918:AINAOT%3E2.0.CO;2

Mellor, G. L., & Yamada, T. (1974). A hierarchy of turbulence closure models for planetary boundary layers. *Journal of the Atmospheric Sciences*, *31*(7), 1791–1806. doi: https://doi.org/10.1175/1520-0469(1974)031%3C1791:AHOTCM%3E2.0.CO;2

Mellor, G. L., & Yamada, T. (1982). Development of a turbulence closure model for geophysical fluid problems. *Reviews of Geophysics*, *20*(4), 851–875. doi: https://doi.org/10.1029/RG020i004p00851

Mesinger, F., & Janjić, Z. I. (1985). Problems and numerical methods of the incorporation of mountains in atmospheric models. *Lectures in Applied Mathematics*, *22*, 81–120.

Müller, M. D., Masbou, M., & Bott, A. (2010). Three-dimensional fog forecasting in complex terrain. *Quarterly Journal of the Royal Meteorological Society*,

136(653), 2189–2202. doi: https://doi.org/10.1002/qj.705

Philip, A., Bergot, T., Bouteloup, Y., & Bouyssel, F. (2016). The impact of vertical resolution on fog forecasting in the kilometric-scale model AROME: A case study and statistics. *Weather and Forecasting*, *31*(5), 1655–1671. doi: https://doi.org/10.1175/WAF-D-16-0074.1

Phillips, N. A. (1957). A coordinate system having some special advantages for numerical forecasting. *Journal of Meteorology*, *14*(2), 184–185. doi: https://doi.org/10.1175/1520-0469(1957)014%3C0184:ACSHSS%3E2.0.CO;2

Pithani, P., Ghude, S. D., Chennu, V. N., Kulkarni, R. G., Steeneveld, G.-J., Sharma, A., ... Madhavan, R. (2019). WRF model prediction of a dense fog event occurred during the Winter Fog Experiment (WIFEX). *Pure and Applied Geophysics*, *176*(4), 1827–1846. doi: https://doi.org/10.1007/s00024-018-2053-0

Raschendorfer, M. (2001). The new turbulence parameterization of LM. *COSMO Newsletter*, *1*, 89–97.

Raymond, W. H. (1988). High-order low-pass implicit tangent filters for use in finite area calculations. *Monthly Weather Review*, *116*(11), 2132–2141. doi: https://doi.org/10.1175/1520-0493(1988)116%3C2132:HOLPIT%3E2.0.CO;2

Reinhardt, T., & Seifert, A. (2006). A three-category ice scheme for the LMK. *COSMO Newsletter*, *6*, 115–120.

Ritter, B., & Geleyn, J.-F. (1992). A comprehensive radiation scheme for numerical weather prediction models with potential applications in climate simulations. *Monthly Weather Review*, *120*(2), 303–325. doi: https://doi.org/10.1175/1520-0493(1992)120%3C0303:ACRSFN%3E2.0.CO;2

Román-Cascón, C., Yagüe, C., Steeneveld, G.-J., Morales, G., Arrillaga, J. A., Sastre, M., & Maqueda, G. (2019). Radiation and cloud-base lowering fog events: Observational analysis and evaluation of WRF and HARMONIE. *Atmospheric Research*, *229*, 190–207. doi: https://doi.org/10.1016/j.atmosres.2019.06.018

Schär, C., Leuenberger, D., Fuhrer, O., Lüthi, D., & Girard, C. (2002). A new terrain-following vertical coordinate formulation for atmospheric prediction models. *Monthly Weather Review*, *130*(10), 2459–2480. doi: https://doi.org/10.1175/1520-0493(2002)130%3C2459:ANTFVC%3E2.0.CO;2

Schneider, W., & Bott, A. (2014). On the time-splitting errors of one-dimensional

advection schemes in numerical weather prediction models; a comparative study. *Quarterly Journal of the Royal Meteorological Society*, *140*(684), 2321–2329. doi: https://doi.org/10.1002/qj.2301

Schraff, C., & Hess, R. (2012). A description of the nonhydrostatic regional COSMO-model, Part III: Data assimilation. *COSMO Documentation*. doi: 10.5676/DWDpub/nwv/cosmo-doc5.00III

Simmons, A. J., & Burridge, D. M. (1981). An energy and angular-momentum conserving vertical finite-difference scheme and hybrid vertical coordinates. *Monthly Weather Review*, *109*(4), 758–766. doi: https://doi.org/10.1175/1520-0493(1981)109%3C0758:AEAAMC%3E2.0.CO;2

Sommeria, G., & Deardorff, J. (1977). Subgrid-scale condensation in models of non-precipitating clouds. *Journal of the Atmospheric Sciences*, *34*(2), 344–355. doi: https://doi.org/10.1175/1520-0469(1977)034%3C0344:SSCIMO%3E2.0.CO;2

Steeneveld, G.-J., & de Bode, M. (2018). Unravelling the relative roles of physical processes in modelling the life cycle of a warm radiation fog. *Quarterly Journal of the Royal Meteorological Society*, *144*(714), 1539–1554. doi: https://doi.org/10.1002/qj.3300

Steppeler, J., Doms, G., Schättler, U., Bitzer, H., Gassmann, A., Damrath, U., & Gregoric, G. (2003). Meso-gamma scale forecasts using the nonhydrostatic model LM. *Meteorology and Atmospheric Physics*, *82*(1-4), 75–96. doi: https://doi.org/10.1007/s00703-001-0592-9

Szintai, B., Bazile, E., & Seity, Y. (2014). Improving wintertime low cloud forecasts in AROME: Sensitivity experiments and microphysics tuning. *ALADIN-HIRLAM Newsletter*, *3*, 45–58.

Tardif, R. (2007). The impact of vertical resolution in the explicit numerical forecasting of radiation fog: A case study. *Pure and Applied Geophysics*, *164*, 1221–1240. doi: https://doi.org/10.1007/978-3-7643-8419-7_8

Tudor, M. (2010). Impact of horizontal diffusion, radiation and cloudiness parameterization schemes on fog forecasting in valleys. *Meteorology and Atmospheric Physics*, *108*(1-2), 57–70. doi: https://doi.org/10.1007/s00703-010-0084-x

Wanner, H., & Furger, M. (1990). The bise – Climatology of a regional wind north of the Alps. *Meteorology and Atmospheric Physics*, *43*(1-4), 105–115. doi: https://doi.org/10.1007/BF01028113

Westerhuis, S., Fuhrer, O., Bhattacharya, R., Schmidli, J., & Bretherton, C. (2020). Effects of terrain-following vertical coordinates on simulation of stratus clouds in numerical weather prediction models. *Quarterly Journal of the Royal Meteorological Society*. doi: https://doi.org/10.1002/qj.3907

Westerhuis, S., Fuhrer, O., Cermak, J., & Eugster, W. (2020). Identifying the key challenges for fog and low stratus forecasting in complex terrain. *Quarterly Journal of the Royal Meteorological Society*. doi: https://doi.org/10.1002/qj.3849

Wicker, L. J., & Skamarock, W. C. (2002). Time–splitting methods for elastic models using forward time schemes. *Monthly Weather Review*, *130*(8), 2088–2097. doi: https://doi.org/10.1175/1520-0493(2002)130%3C2088:TSMFEM%3E2.0.CO;2

Wilson, T. H., & Fovell, R. G. (2018). Modeling the evolution and life cycle of radiative cold pools and fog. *Weather and Forecasting*, *33*(1), 203–220.

Zängl, G. (2002). An improved method for computing horizontal diffusion in a sigma-coordinate model and its application to simulations over mountainous topography. *Monthly Weather Review*, *130*(5), 1423–1432. doi: https://doi.org/10.1175/1520-0493(2002)130%3C1423:AIMFCH%3E2.0.CO;2

Zängl, G. (2003). A generalized sigma-coordinate system for the MM5. *Monthly weather review*, *131*(11), 2875–2884. doi: https://doi.org/10.1175/1520-0493(2003)131⟨2875:AGSSFT⟩2.0.CO;2

Zängl, G. (2012). Extending the numerical stability limit of terrain-following coordinate models over steep slopes. *Monthly Weather Review*, *140*(11), 3722–3733. doi: https://doi.org/10.1175/MWR-D-12-00049.1